Higgs production in e and real gamma collision

Ken Sasaki (Yokohama National U.)

In collaboration with

H. Watanabe (KEK)

Y. Kurihara (KEK)

T. Uematsu (Kyoto U.)

Physics Letters B (2013) arXiv:1311.1601[hep-ph]

Full paper in preparation

Workshop on High-energy QCD and nucleon structure

March 7-8, 2014, KEK Tokai campus

Outline

1. Introduction and motivations
2. Higgs production in e and real γ collision in SM
3. Two-photon and Z-photon fusion diagrams
4. W-related and Z-related diagrams
5. Differential cross section
6. Numerical analysis
7. Summary

1. Introduction and motivations

- A Higgs particle was found at the LHC

  Is it the SM Higgs boson , a SUSY Higgs boson,

  a Higgs boson of a different model?

- Future linear collider : ILC
  - $\mathbf{e^+e^-}$ collider: $\sqrt{\mathbf{s}} = \mathbf{250}\ \mathrm{GeV} \cdots$
  - It may be constructed in Japan.

- Before e+ beams are ready,

  other options are possible:
  - an $\mathbf{e^-e^-}$ option
  - an $\mathbf{e^-}\gamma$ option

    use one e- beam to produce high energy photons

γe^- collider based on e^-e^-

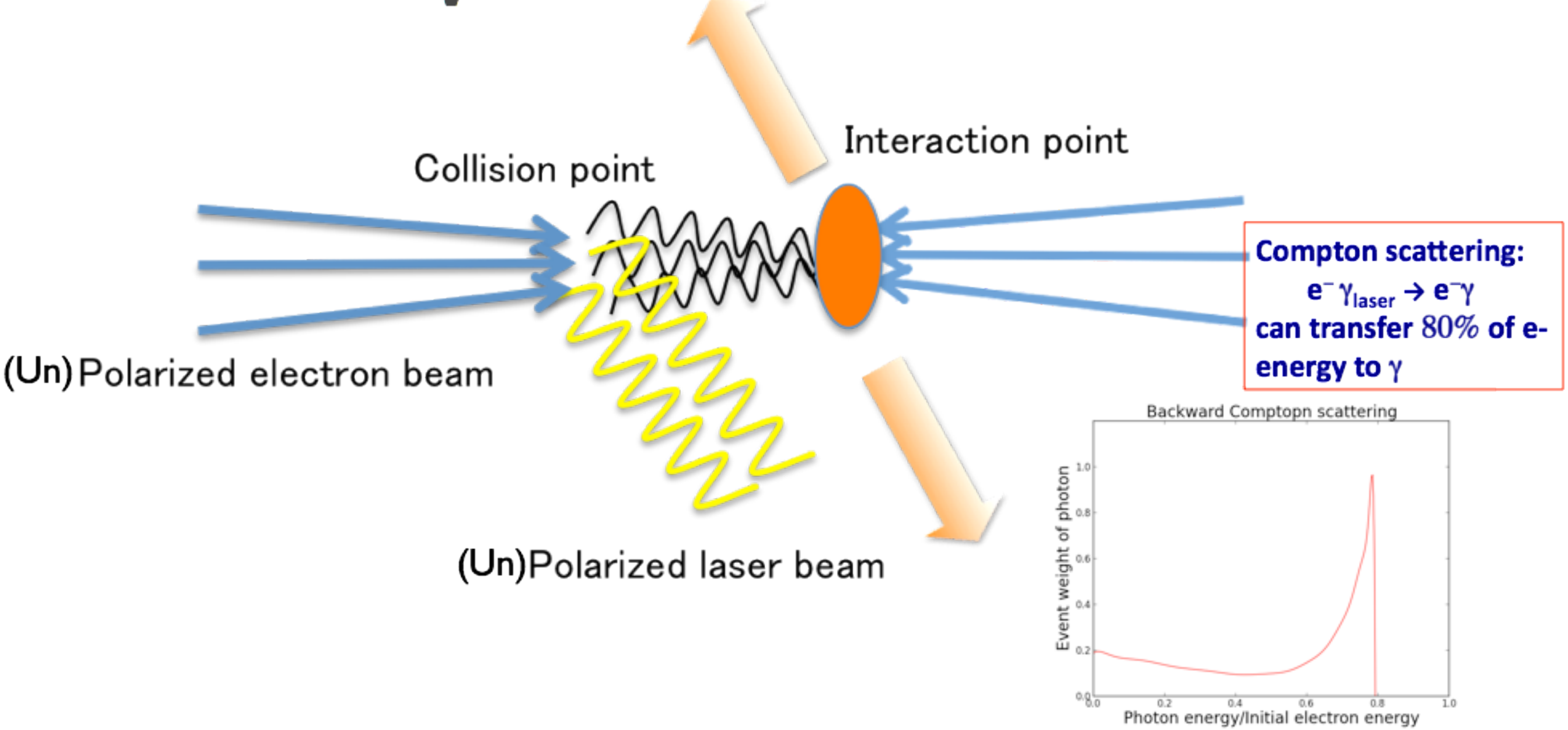

Good test for combining photon science & particle physics!!

1. Introduction and motivations

- In two-photon fusion process for Higgs production in eγ collision, we may observe the transition form factor of Higgs

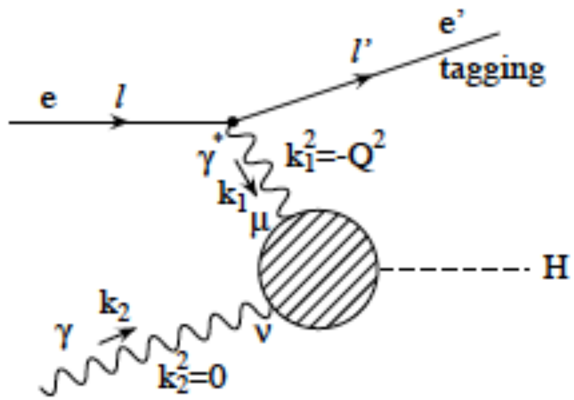

in analogy of the $\gamma^*\gamma \to \pi^0$ transition form factor observed at BaBar and Belle

1. Introduction and motivations

- The $\gamma^*\gamma \to \pi^0$ transition form factor $F(Q^2)$ observed at BaBar and Belle

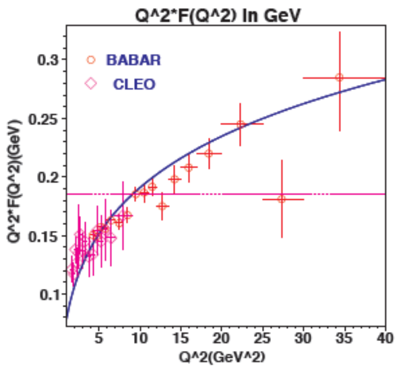

BaBar

不一致

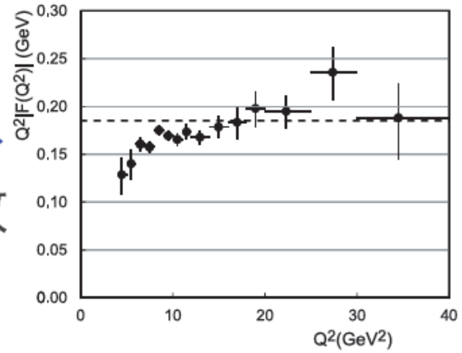

Belle

Lepage and Brodsky, PR D9 (1980) 2157
Barbar Collaboration, PR D80 (2009) 052002
Belle Collaboration, PR D86 (2012) 092007

2 Higgs production in e- and real γ collision in SM

- Higgs are produced by loop diagrams

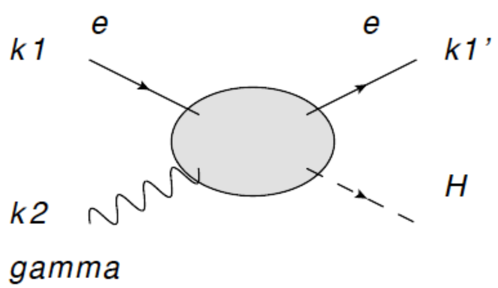

At one-loop level

$\gamma\gamma$-fusion diagrams
$\mathbf{Z}\gamma$-fusion diagrams
W-related diagrams
Z-related diagrams

$$k_1^2 = {k_1'}^2 = m_e^2 = 0\ ; \quad p_h^2 = m_h^2,$$

$$\begin{aligned} s &= (k_1 + k_2)^2 = 2k_1 \cdot k_2\ , \quad t = (k_1 - k_1')^2 = -2k_1 \cdot k_1' = q^2, \\ u &= (k_1 - p_h)^2 = (k_1' - k_2)^2 = -2k_1' \cdot k_2 = m_h^2 - s - t \\ k_2^2 &= 0\ , \qquad k_2^\beta\ \epsilon(k_2)_\beta = 0 \end{aligned}$$

2 Higgs production in e- and real γ collision in SM

- Calculation is done in unitary gauge
- Use of FeynCalc, PaVeReduce[Oneloop[p,-----]]
- Amplitudes are expressed in analytical form

Denner, Nierste, Scharf (1991)

Keith Ellis, Zanderighi (2008)

Denner, Dittmaier (2010)

3. Two-photon and Z-photon fusion diagrams

$e \cdot e \cdot \gamma$ coupling : $i(-e)\gamma_\mu$

$t \cdot t \cdot \gamma$ coupling : $i(q_t e)\gamma_\mu$

$e \cdot e \cdot Z$ coupling : $i\dfrac{g}{4\cos\theta_W}\gamma_\mu(f_{Ze}+\gamma_5)$ with $f_{Ze}=-1+4\sin^2\theta_W$

$t \cdot t \cdot Z$ coupling : $i\,\dfrac{g}{4\cos\theta_W}\gamma_\mu\,[f_{Zt}-\gamma_5]$ with $f_{Zt}=1-\dfrac{8}{3}\sin^2\theta_W$

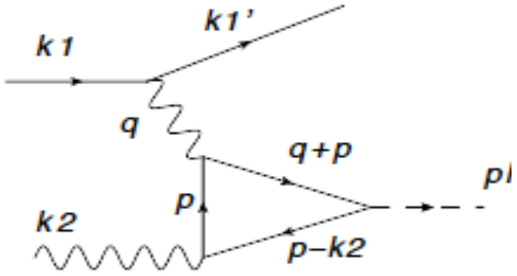

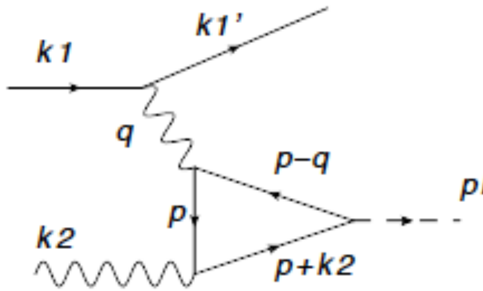

Higgs $\cdot\, t \cdot t$ coupling : $-i\,\dfrac{gm_t}{2m_W}$

Higgs $\cdot\, W \cdot W$ coupling : $igm_W\, g_{\mu\nu}$

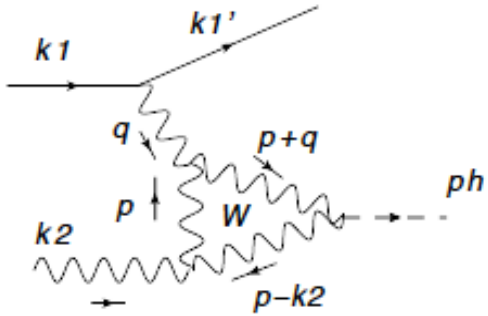

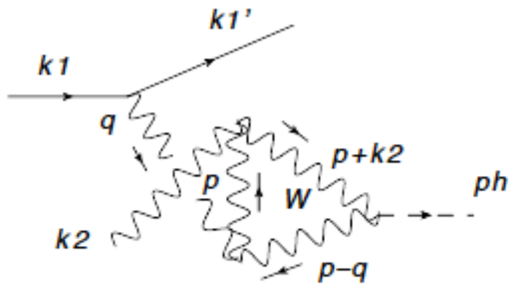

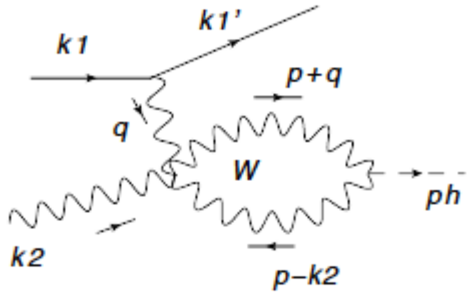

$Z_\mu(k_1)$-$W^+_\nu(k_2)$-$W^-_\lambda(k_3)$ coupling: $-ig\cos\theta_W\left[(k_1-k_2)_\lambda g_{\mu\nu}+(k_2-k_3)_\mu g_{\nu\lambda}+(k_3-k_1)_\nu g_{\lambda\mu}\right]$

A_μ-Z_ν-W^+_α-W^-_β coupling: $-ieg\cos\theta_W\left[2g_{\mu\nu}g_{\alpha\beta}-g_{\mu\alpha}g_{\nu\beta}-g_{\mu\beta}g_{\nu\alpha}\right]$

3. Two-photon and Z-photon fusion diagrams

- Contribution of two-photon fusion diagrams

$$A_{\gamma\gamma} = \left(\frac{e^3 g}{16\pi^2}\right)\left[\overline{u}(k_1')\gamma_\mu u(k_1)\right]\frac{1}{t}\left(g^{\mu\beta} - \frac{2k_2^\mu q^\beta}{m_h^2 - t}\right)\epsilon_\beta(k_2)\ F_{\gamma\gamma}$$

$$F_{\gamma\gamma} = \frac{2m_t^2}{m_W} N_c Q_t^2\ S_{(T)}^{\gamma\gamma}(t, m_t^2, m_h^2) - m_W\, S_{(W)}^{\gamma\gamma}(t, m_W^2, m_h^2)$$

  - Top quark loops:

$$S_{(T)}^{\gamma\gamma}(t, m_t^2, m_h^2) = 2 - \frac{2t}{m_h^2 - t} B_0(t; m_t^2, m_t^2) + \frac{2t}{m_h^2 - t} B_0(m_h^2; m_t^2, m_t^2) + \left\{4m_t^2 - m_h^2 + t\right\} C_0(m_h^2, 0, t; m_t^2, m_t^2, m_t^2)$$

$$B_0(p^2; m_1^2, m_2^2) \equiv \frac{(2\pi\mu)^{4-n}}{i\pi^2}\int \frac{d^n k}{\left[k^2 - m_1^2\right]\left[(k+p)^2 - m_2^2\right]}$$

$$C_0(p_1^2, p_2^2, p_3^2; m_1^2, m_2^2, m_3^2) \equiv \frac{(2\pi\mu)^{4-n}}{i\pi^2}\int \frac{d^n k}{\left[k^2 - m_1^2\right]\left[(k+p_1)^2 - m_2^2\right]\left[(k+p_1+p_2)^2 - m_3^2\right]}$$

  - W boson loops:

$$S_{(W)}^{\gamma\gamma}(t, m_W^2, m_h^2) = 6 + \frac{m_h^2 - t}{m_W^2} - \frac{m_h^2 t}{2m_W^4} + \frac{t\left(12m_W^4 + 2m_W^2\left(m_h^2 - t\right) - m_h^2 t\right)}{2m_W^4\left(m_h^2 - t\right)}\left[B_0(m_h^2; m_W^2, m_W^2) - B_0(t; m_W^2, m_W^2)\right] + \left\{\frac{t\left(m_h^2 - 2t\right)}{m_W^2} + 12m_W^2 - 6m_h^2 + 6t\right\} C_0(m_h^2, 0, t; m_W^2, m_W^2, m_W^2)$$

3. Two-photon and Z-photon fusion diagrams

- Contribution of Z-photon fusion diagrams

$$A_{Z\gamma} = \left(\frac{eg^3}{16\pi^2}\right)\left[\overline{u}(k_1')\gamma_\mu\left(f_{Ze}+\gamma_5\right)u(k_1)\right]\frac{1}{t-m_Z^2}\left(g^{\mu\beta}-\frac{2k_2^\mu q^\beta}{m_h^2-t}\right)\epsilon_\beta(k_2)\; F_{Z\gamma}$$

$$F_{Z\gamma} = -\frac{m_t^2}{8m_W\cos^2\theta_W}N_cQ_tf_{Zt}S^{Z\gamma}_{(T)}(t,m_t^2,m_h^2)+\frac{m_W}{4}S^{Z\gamma}_{(W)}(t,m_W^2,m_h^2)$$

  - Top quark loops: $S^{Z\gamma}_{(T)}(t,m_t^2,m_h^2) = S^{\gamma\gamma}_{(T)}(t,m_t^2,m_h^2)$
  - W boson loops: $S^{Z\gamma}_{(W)}(t,m_W^2,m_h^2) = S^{\gamma\gamma}_{(W)}(t,m_W^2,m_h^2)$

The contribution of two-photon and Z-photon fusion diagrams have the same transition form factors

4. W-related and Z-related diagrams

- GRACE gives other contributions to Higgs production in e - γ collision

$e \cdot \nu \cdot W$ coupling : $i\frac{g}{2\sqrt{2}}\gamma_\mu(1-\gamma_5)$

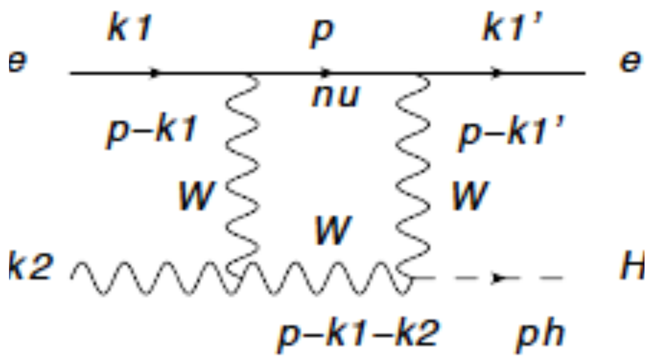

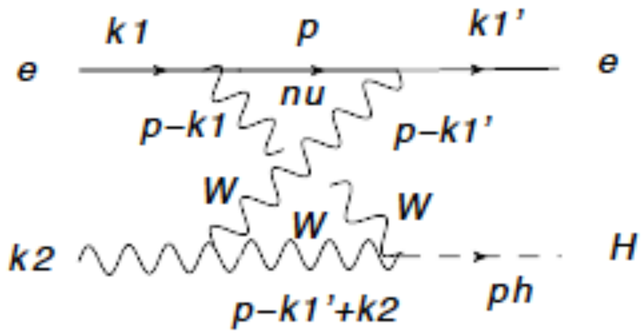

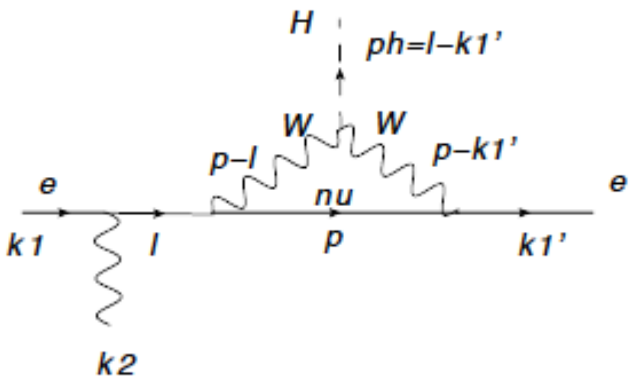

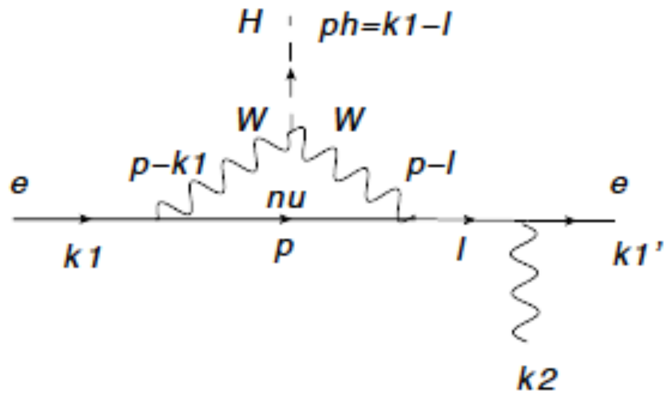

4. W-related and Z-related diagrams

$e \cdot e \cdot Z$ coupling : $\quad i\dfrac{g}{4\cos\theta_W}\gamma_\mu(f_{Z_e}+\gamma_5) \quad$ with $\quad f_{Z_e} = -1 + 4\sin^2\theta_W$

Higgs $\cdot Z \cdot Z$ coupling : $\quad i\dfrac{g m_Z}{\cos\theta_W} g_{\mu\nu}$

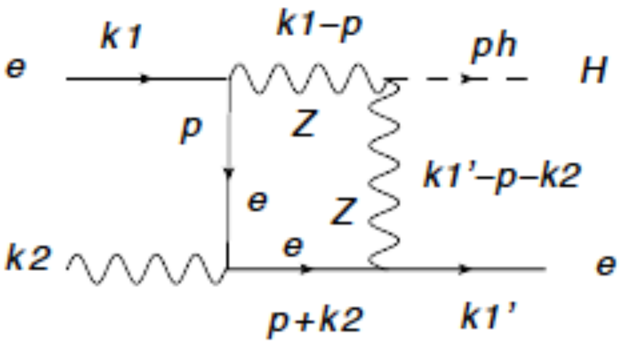

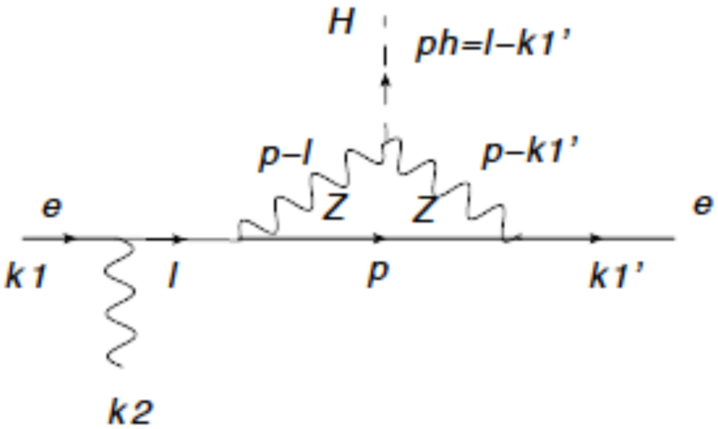

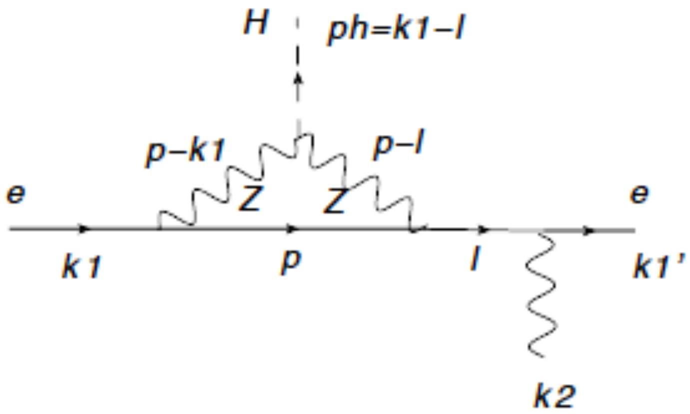

4. W-related and Z-related diagrams

- Contribution of W-related diagrams

$$A_{W\nu_e} = \left(\frac{eg^3}{16\pi^2}\right)\frac{m_W}{4}\left[\overline{u}(k_1')\, F_{(W\nu_e)\beta}\, (1-\gamma_5)u(k_1)\right]\epsilon(k_2)^\beta$$

$$F_{(W\nu_e)\beta} = \left(\frac{2k_{1_\beta}\not{k}_2}{s} - \gamma_\beta\right)S^{W\nu_e}_{(k_1)}(s,t,m_h^2,m_W^2) + \left(\frac{2k'_{1_\beta}\not{k}_2}{u} + \gamma_\beta\right)S^{W\nu_e}_{(k_1')}(s,t,m_h^2,m_W^2)$$

where

Note: $S^{W\nu_e}_{(k_1')} \to 0 \quad \text{as} \quad u \to 0$

$S^{W\nu_e}_{(k_1)}(s,t,m_h^2,m_W^2)$ and $S^{W\nu_e}_{(k_1')}(s,t,m_h^2,m_W^2)$

: expressed as a linear combination of

$$B_0(s;0,m_W^2) \qquad B_0(u;0,m_W^2) \qquad B_0\left(t;m_W^2,m_W^2\right) \qquad B_0\left(m_h^2;m_W^2,m_W^2\right)$$

$$C_0\left(0,0,s;m_W^2,m_W^2,0\right) \quad C_0\left(0,0,u;m_W^2,m_W^2,0\right) \quad C_0\left(0,0,t;m_W^2,0,m_W^2\right)$$

$$C_0\left(0,s,m_h^2;m_W^2,0,m_W^2\right) \quad C_0\left(0,u,m_h^2;m_W^2,0,m_W^2\right) \quad C_0\left(0,t,m_h^2;m_W^2,m_W^2,m_W^2\right)$$

$$D_0\left(0,0,0,m_h^2;s,t;m_W^2,m_W^2,0,m_W^2\right) \qquad D_0\left(0,0,0,m_h^2;t,u;m_W^2,0,m_W^2,m_W^2\right)$$

- When the initial electron is right-handed, $A_{W\nu_e} = 0$

4. W-related and Z-related diagrams

- Contribution of Z-related diagrams

$$A_{Ze} = \left(\frac{eg^3}{16\pi^2}\right)\left(-\frac{m_Z}{16\cos^3\theta_W}\right) \times \left[\overline{u}(k_1')\ F_{(Ze)\beta}\ (f_{Ze}+\gamma_5)^2 u(k_1)\right]\epsilon(k_2)^\beta$$

$$F_{(Ze)\beta} = \left(\frac{2k_{1_\beta}\not{k}_2}{s} - \gamma_\beta\right)S^{Ze}_{(k_1)}(s,t,m_h^2,m_Z^2) + \left(\frac{2k'_{1_\beta}\not{k}_2}{u} + \gamma_\beta\right)S^{Ze}_{(k_1')}(s,t,m_h^2,m_Z^2)$$

where

Note: $S^{Ze}_{(k_1')} \to 0$ as $u \to 0$

$S^{Ze}_{(k_1)}(s,t,m_h^2,m_Z^2)$ and $S^{Ze}_{(k_1')}(s,t,m_h^2,m_Z^2)$

: expressed as a linear combination of

$B_0(s;0,m_Z^2)$ $\quad B_0(u;0,m_Z^2)$ $\quad B_0\left(m_h^2;m_Z^2,m_Z^2\right)$

$C_0\left(0,0,s;m_Z^2,0,0\right)$ $\quad C_0\left(0,0,u;m_Z^2,0,0\right)$ $\quad C_0\left(0,s,m_h^2;m_Z^2,0,m_Z^2\right)$ $\quad C_0\left(0,u,m_h^2;m_Z^2,0,m_Z^2\right)$

$D_0\left(0,0,0,m_h^2;s,u;m_Z^2,0,0,m_Z^2\right)$

- Collinear divergences appear in $C_0\left(0,0,s;m_Z^2,0,0\right)$ $C_0\left(0,0,u;m_Z^2,0,0\right)$ $D_0\left(0,0,0,m_h^2;s,u;m_Z^2,0,0,m_Z^2\right)$

  but they are cancel out when they are added

4. W-related and Z-related diagrams

$$C_0(0,0,s;m_Z^2,0,0) = -\left(\frac{4\pi\mu^2}{m_Z^2}\right)^{\epsilon}\frac{1}{s}\left\{\frac{1}{\epsilon}\Big[\log(s_Z-1)-i\pi\Big]-\frac{1}{2}\Big[\log(s_Z-1)-i\pi\Big]^2\right.$$
$$\left.-\mathrm{Li}_2\left(\frac{s_Z-1}{s_Z}\right)-\frac{1}{2}\log^2\left(\frac{s_Z}{s_Z-1}\right)+\frac{\pi^2}{3}-i\pi\log\left(\frac{s_Z}{s_Z-1}\right)\right\}$$
$$C_0(0,0,u;m_Z^2,0,0) = -\left(\frac{4\pi\mu^2}{m_Z^2}\right)^{\epsilon}\frac{1}{u}\left\{\frac{1}{\epsilon}\log(1-u_Z)+\mathrm{Li}_2\left(\frac{-u_Z}{1-u_Z}\right)-\frac{1}{2}\log^2(1-u_Z)\right\}$$

$$s_Z=\frac{s}{m_Z^2},\quad u_Z=\frac{u}{m_Z^2},\quad h_Z=\frac{m_h^2}{m_Z^2}$$

$$x_{Z_+}=\frac{1}{2}\left(1+i\sqrt{\frac{4}{h_Z}-1}\right)$$
$$x_{Z_-}\equiv\frac{1}{2}\left(1-i\sqrt{\frac{4}{h_Z}-1}\right)$$

$$D_0(0,0,0,m_h^2;s,u;m_Z^2,0,0,m_Z^2) = D_0(0,0,m_h^2,0;s,u;0,0,m_Z^2,m_Z^2)$$
$$=\frac{1}{su-m_Z^2(s+u)}\left\{\left(\frac{4\pi\mu^2}{m_Z^2}\right)^{\epsilon}e^{-\epsilon\gamma_E}\times\frac{1}{\epsilon}\Big[-\Big[\log(s_Z-1)-i\pi\Big]-\log(1-u_Z)\Big]\right.$$
$$+2\mathrm{Li}_2\left(\frac{s_Z-1}{s_Z}\right)-2\mathrm{Li}_2\left(-\frac{u_Z}{1-u_Z}\right)-2\mathrm{Li}_2\left(\frac{1}{(1-s_Z)(1-u_Z)}\right)$$
$$+\mathrm{Li}_2\left(-\frac{x_{Z_+}}{x_{Z_-}(1-s_Z)}\right)+\mathrm{Li}_2\left(-\frac{x_{Z_-}}{x_{Z_+}(1-s_Z)}\right)+\mathrm{Li}_2\left(1+\frac{x_{Z_+}(1-u_Z)}{x_{Z_-}}\right)+\mathrm{Li}_2\left(1+\frac{x_{Z_-}(1-u_Z)}{x_{Z_+}}\right)$$
$$+\log^2\left(\frac{s_Z}{s_Z-1}\right)+2\log\Big((s_Z-1)(1-u_Z)\Big)\log\left(\frac{s_Z+u_Z-u_Zs_Z}{(s_Z-1)(1-u_Z)}\right)+2\log(s_Z-1)\log(1-u_Z)$$
$$+\log^2(1-u_Z)+\log\left(1+\frac{x_{Z_+}}{x_{Z_-}(1-s_Z)}\right)\left\{\log\left(-\frac{x_{Z_+}}{x_{Z_-}}\right)-\log(s_Z-1)\right\}$$
$$+\log\left(1+\frac{x_{Z_-}}{x_{Z_+}(1-s_Z)}\right)\left\{\log\left(-\frac{x_{Z_-}}{x_{Z_+}}\right)-\log(s_Z-1)\right\}$$
$$+i\pi\left[2\log\left(\frac{s_Z}{s_Z+u_Z-u_Zs_Z}\right)+\log\left(1+\frac{x_{Z_+}}{x_{Z_-}(1-s_Z)}\right)+\log\left(1+\frac{x_{Z_-}}{x_{Z_+}(1-s_Z)}\right)\right]$$
$$\left.-\frac{2\pi^2}{3}\right\} \qquad \text{(B3}$$

- They appear in combination of $\left\{sC_0\left(0,0,s;m_Z^2,0,0\right)+uC_0\left(0,0,u;m_Z^2,0,0\right)\right.$
$\left.+[m_Z^2(s+u)-su]D_0\left(0,0,0,m_h^2;s,u;m_Z^2,0,0,m_Z^2\right)\right\}$

5. Differential cross section

- Linear Collider : good polarizations for the initial colliding beams

  Initial electron polarization: $P_e = \pm 1$

  Initial photon polarization: $P_\gamma = \pm 1$

- Differential cross section

$$\frac{d\sigma_{(e\gamma \to eH)}(P_e, P_\gamma)}{dt} = \frac{1}{16\pi s^2} \times \left\{ \sum_{\text{final electron spin}} |A(P_e, P_\gamma)|^2 \right\}$$

$$A(P_e, P_\gamma) = A_{\gamma\gamma}(P_e, P_\gamma) + A_{Z\gamma}(P_e, P_\gamma) + A_{W\nu_e}(P_e, P_\gamma) + A_{Ze}(P_e, P_\gamma)$$

- Angular momentum conservation in forward and backward directions
  - In the massless limit of electron, its helicity is conserved

$A(P_e, P_\gamma)$ vanishes at $\theta = 0$ $\quad A(P_e, P_\gamma) \propto t$

$A(P_e, P_\gamma)$ with $P_e P_\gamma = -1$ vanishes at $\theta = \pi$ $\quad A(P_e P_\gamma = -1) \to 0$ as $u \to 0$

5. Differential cross section

- To obtain $A(P_e, P_\gamma)$:

$$u(k_1) \to \frac{1 + P_e \gamma_5}{2} u(k_1)$$

$$\epsilon(k_2, \pm 1)^*_\alpha \epsilon(k_2, \pm 1)_\beta = -\frac{1}{2} g_{\alpha\beta} \pm \frac{i}{2} \left(g_{\alpha 1} g_{\beta 2} - g_{\alpha 2} g_{\beta 1} \right)$$

In the frame where the initial photon is moving in the z-direction

- Contributions from $\gamma\gamma$ fusion, $Z\gamma$ fusion, "W-ν_e" and "Z-e" diagrams

$$\frac{d\sigma_{(\gamma\gamma)}(P_e, P_\gamma)}{dt} = \frac{1}{16\pi \; s^2} \times \left\{ \sum_{\text{final electron spin}} |A_{\gamma\gamma}(P_e, P_\gamma)|^2 \right\}$$

$$= \frac{1}{16\pi \; s^2} \left(\frac{e^3 g}{16\pi^2} \right)^2 \left(-\frac{1}{t} \right) F_{\gamma\gamma}{}^2 \left\{ \frac{s^2 + u^2}{(s+u)^2} + P_\gamma P_e \left(1 - \frac{2u}{s+u} \right) \right\},$$

5. Differential cross section

$$\frac{d\sigma_{(Z\gamma)}(P_e,P_\gamma)}{dt} = \frac{1}{16\pi\ s^2}\left(\frac{eg^3}{16\pi^2}\right)^2\frac{-t}{(t-m_Z^2)^2}\,{F_{Z\gamma}}^2 \times\left\{(f_{Ze}^2+2P_ef_{Ze}+1)\frac{s^2+u^2}{(s+u)^2}+P_\gamma(P_ef_{Ze}^2+2f_{Ze}+P_e)\left(1-\frac{2u}{s+u}\right)\right\},$$

$$\frac{d\sigma_{(W\nu_e)}(P_e,P_\gamma)}{dt} = \frac{1}{16\pi s^2}\left(\frac{eg^3}{16\pi^2}\right)^2\frac{m_W^2}{8}(-t)(1-P_e)\left\{\left[\left|S_{(k_1)}^{W\nu_e}(s,t,m_h^2,m_W^2)\right|^2+\left|S_{(k_1')}^{W\nu_e}(s,t,m_h^2,m_W^2)\right|^2\right] +P_\gamma\left[-\left|S_{(k_1)}^{W\nu_e}(s,t,m_h^2,m_W^2)\right|^2+\left|S_{(k_1')}^{W\nu_e}(s,t,m_h^2,m_W^2)\right|^2\right]\right\},$$

$$\frac{d\sigma_{(Ze)}(P_e,P_\gamma)}{dt} = \frac{1}{16\pi s^2}\left(\frac{eg^3}{16\pi^2}\right)^2\left(\frac{m_Z}{16\cos^3\theta_W}\right)^2(-t) \times\left\{(f_{Ze}^4+4P_ef_{Ze}^3+6f_{Ze}^2+4P_ef_{Ze}+1)\left[\left|S_{(k_1)}^{Ze}(s,t,m_h^2,m_Z^2)\right|^2+\left|S_{(k_1')}^{Ze}(s,t,m_h^2,m_Z^2)\right|^2\right] +P_\gamma(P_ef_{Ze}^4+4f_{Ze}^3+6P_ef_{Ze}^2+4f_{Ze}+P_e)\left[\left|S_{(k_1)}^{Ze}(s,t,m_h^2,m_Z^2)\right|^2 -\left|S_{(k_1')}^{Ze}(s,t,m_h^2,m_Z^2)\right|^2\right]\right\}.$$

We see $\quad \dfrac{d\sigma_{(W\nu_e)}(P_e=+1)}{dt}=0 \qquad \dfrac{d\sigma(P_eP_\gamma=-1)}{dt}\to 0 \quad \text{as} \quad u\to 0$

6. Numerical analysis

- Parameters

$$m_h = 125 \text{ GeV} , \quad m_t = 173 \text{ GeV} , \quad m_Z = 91 \text{ GeV} , \quad m_W = 80 \text{ GeV}$$

$$\cos\theta_W = \frac{m_W}{m_Z} , \qquad e^2 = 4\pi\alpha_{em} = \frac{4\pi}{128} , \qquad g = \frac{e}{\sin\theta_W} .$$

- t-dependence $\quad \sqrt{s} = 200 \text{ GeV}$

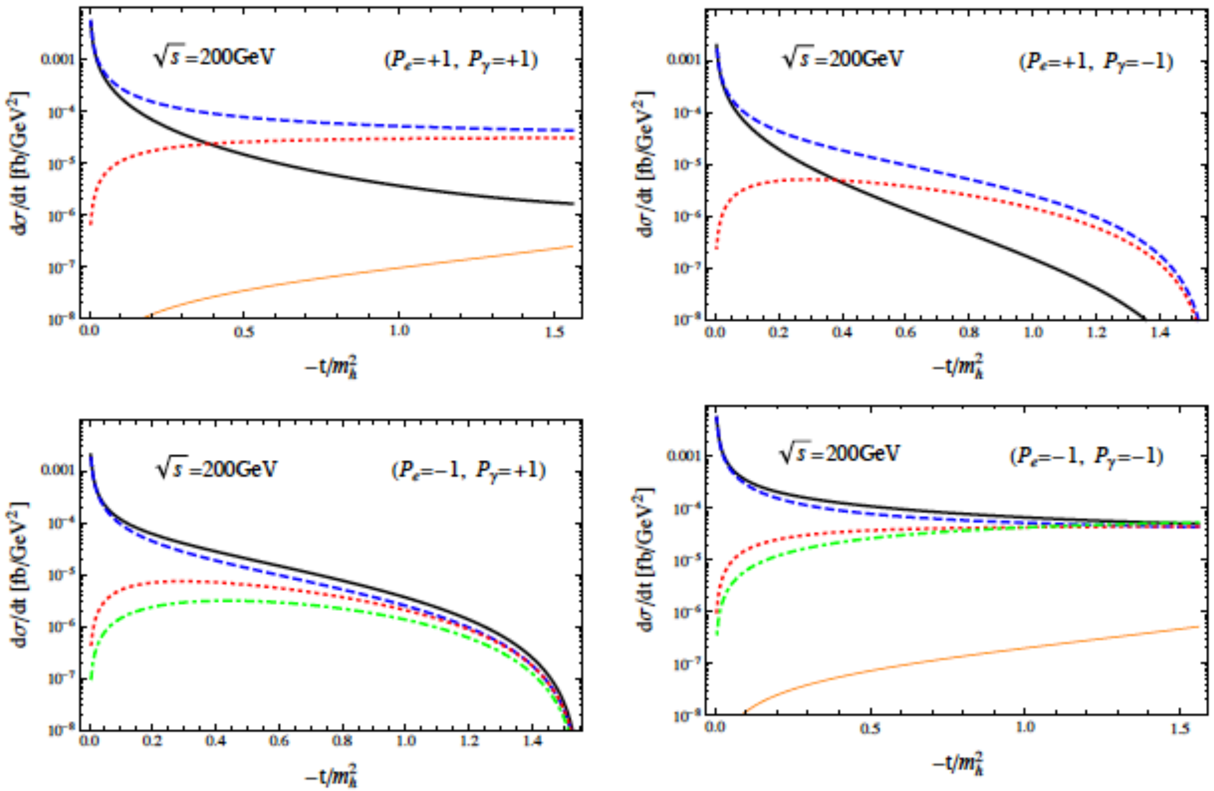

Black	Full
Blue	$\gamma\gamma$
Red	$Z\gamma$
Green	W-related
Orange	Z-related

6. Numerical analysis

- t-dependence $\sqrt{s} = 400\ \text{GeV}$

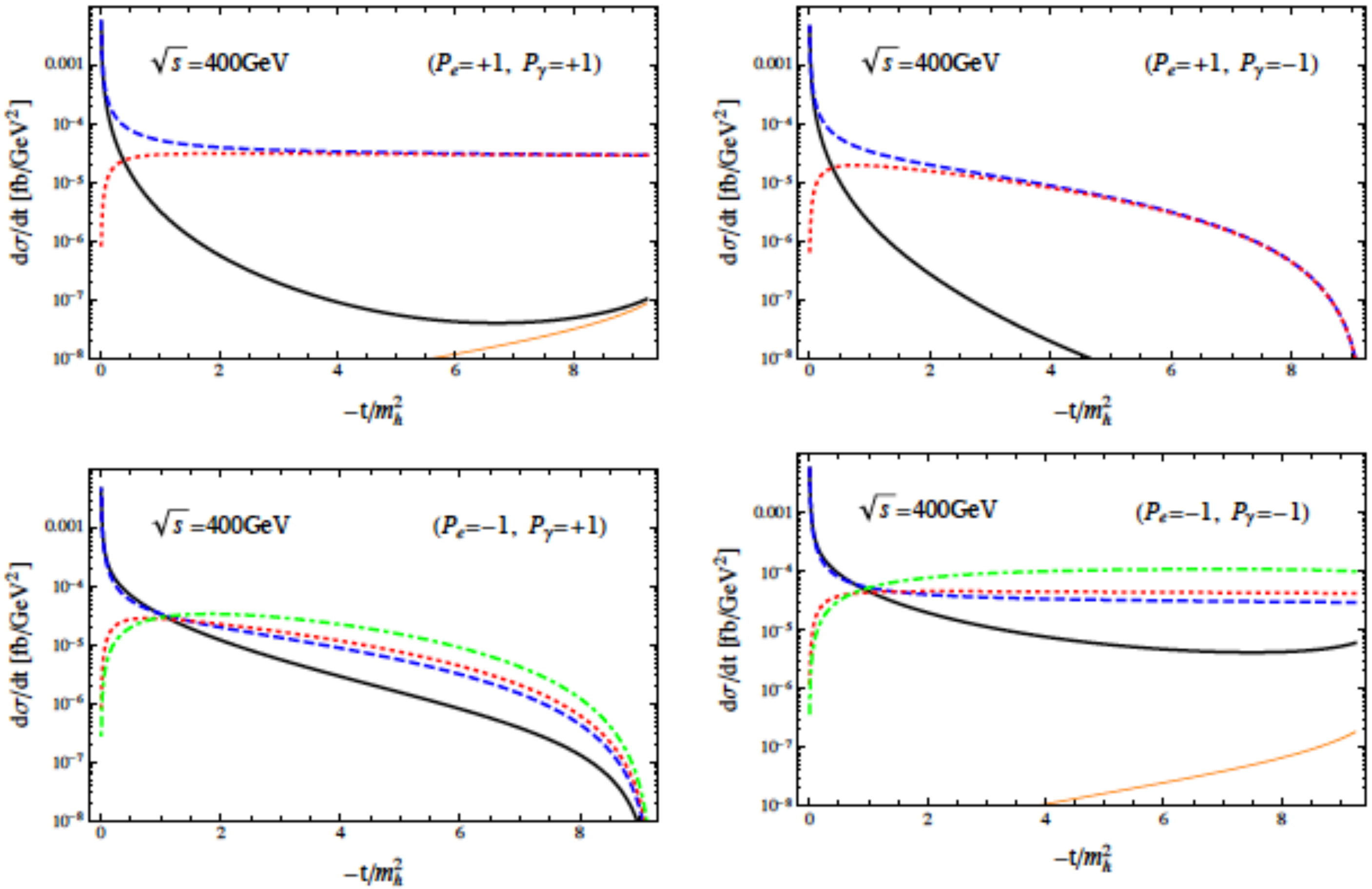

Black	Full
Blue	$\gamma\gamma$
Red	$Z\gamma$
Green	W-related
Orange	Z-related

➢ The contribution from "Z-e" diagrams is negligibly small

6. Numerical analysis

- t-dependence
  - The case $P_e = -1$

    for $-t/m_h^2 \leq 1$, a dominant contribution comes from the $\gamma\gamma$ fusion diagrams

    for $1 < -t/m_h^2 < 1.5$, the contributions from the $\gamma\gamma$ fusion, $Z\gamma$ fusion and "W-ν_e" diagrams becomes the same order

    for $-t/m_h^2 > 1.5$, the contribution from "W-ν_e" diagrams prevails other two

    The interference between $A_{\gamma\gamma}$ and $A_{Z\gamma}$ works constructively

    $A_{\gamma\gamma}$ and $A_{W\nu_e}$ works destructively

  - The case $P_e = +1$

    No contribution from "W-ν_e" diagrams

    The interference between $A_{\gamma\gamma}$ and $A_{Z\gamma}$ works destructively

    Its effect is large even at small $-t/m_h^2$

    $d\sigma_{(e\gamma\to eH)}/dt$ decreases rather rapidly as $-t/m_h^2$ increases

6. Numerical analysis

Higgs production cross section $\sigma_{(e\gamma \to eH)}$

Black	Full
Blue	$\gamma\gamma$
Red	$Z\gamma$
Green	W-related
Orange	Z-related

- s-dependence

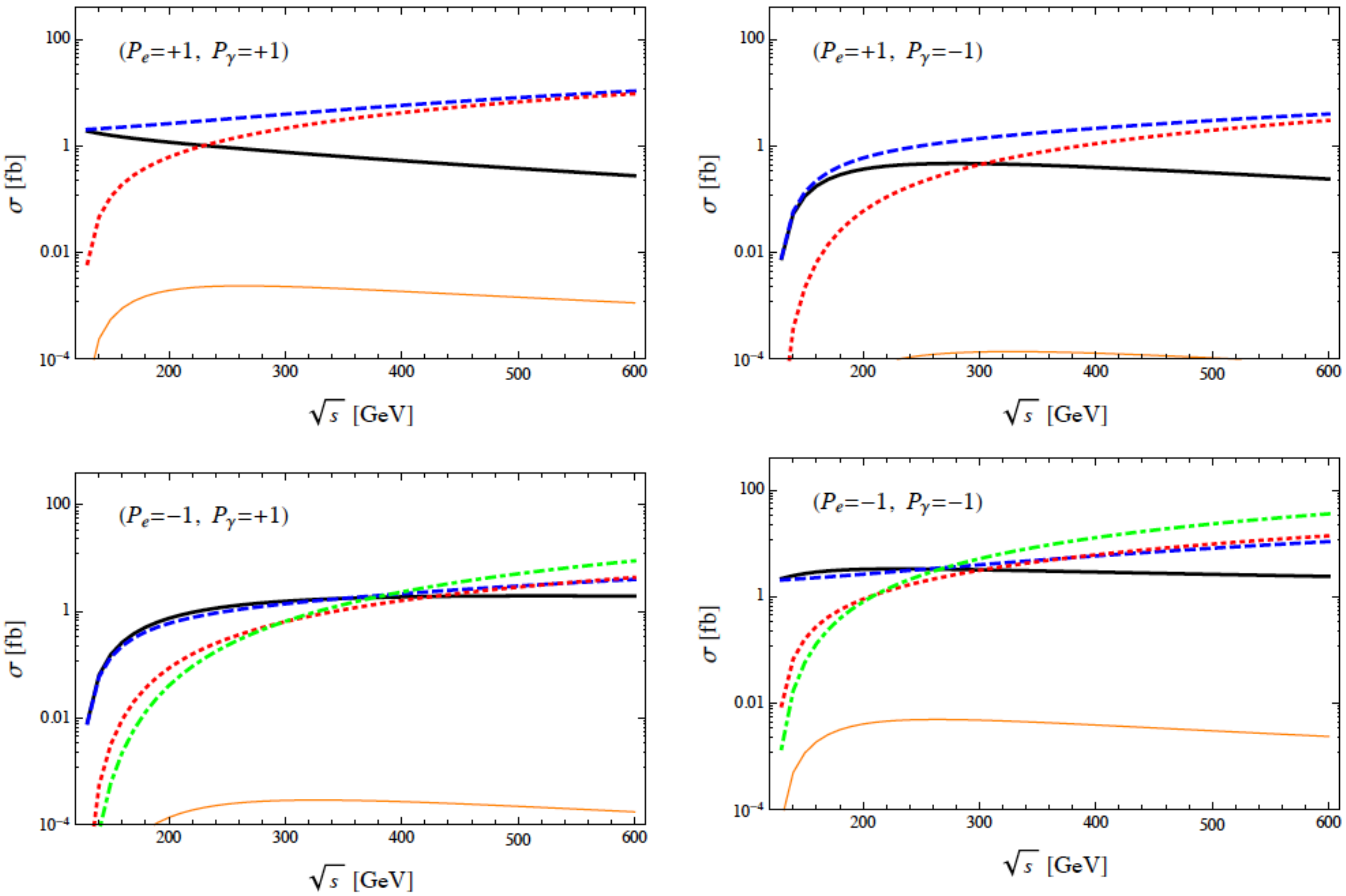

6. Numerical analysis

Higgs production cross section $\sigma_{(e\gamma \to eH)}$

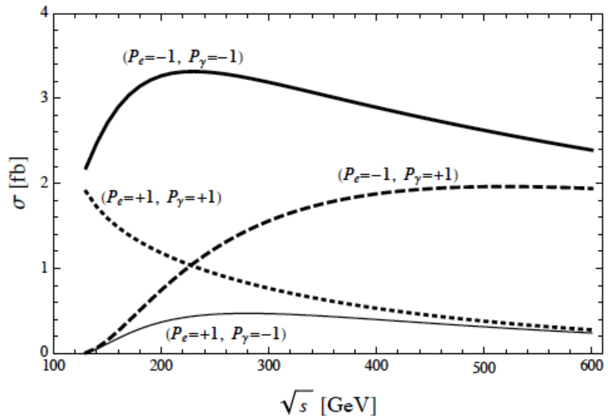

- s-dependence
  - The case $P_e P_\gamma = -1$
    - very small at $\sqrt{s} = 130\ \mathrm{GeV}$
    - rises gradually up to 2 fb for $(P_e = -1, P_\gamma = +1)$
    - increases rather slowly up to 0.4 fb for $(P_e = +1, P_\gamma = -1)$

      due to interference between $A_{\gamma\gamma}$ and $A_{Z\gamma}$
  - The case $P_e P_\gamma = +1$
    - large even at small $\sqrt{s}$
    - rises above 3 fb around $\sqrt{s} = 200\ \mathrm{GeV}$ and then gradually decreases for $(P_e = -1, P_\gamma = -1)$

      due to interference between $A_{W\nu_e}$ and $A_{\gamma\gamma}$
    - decreases as $\sqrt{s}$ increases for $(P_e = +1, P_\gamma = +1)$

      due to interference between $A_{\gamma\gamma}$ and $A_{Z\gamma}$

γe^- collider based on e^-e^-

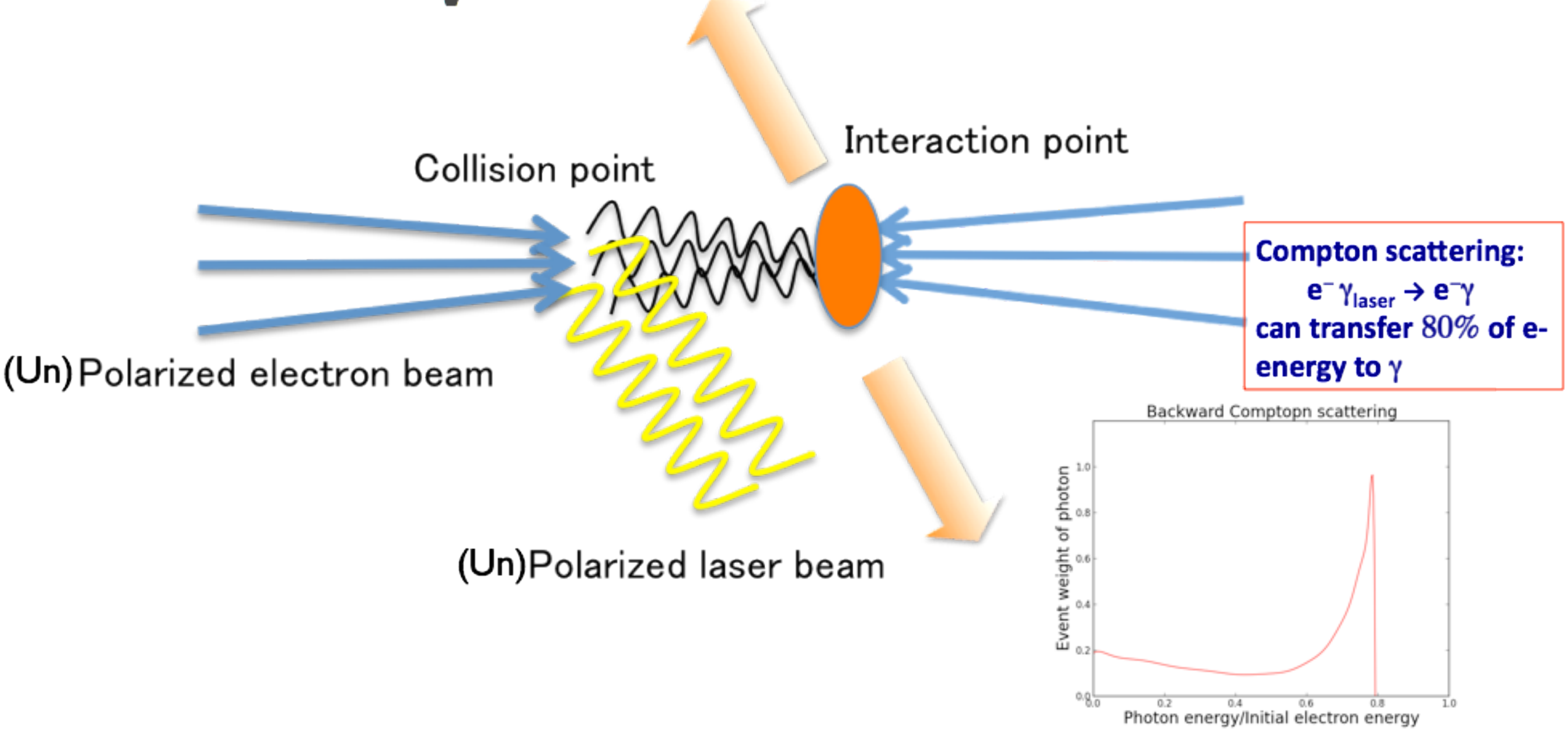

Good test for combining photon science & particle physics!!

6. Numerical analysis

- Higgs production cross section for $e(E_{e1}) + \gamma(yE_{e2}) \to e + H$

  in $e^-(E_{e1})e^-(E_{e2})$ collider

$$\sigma_{e\gamma\ \mathrm{collision}}(s_{ee}, E_{\mathrm{Laser}}, P_{e1}, P_{e2}, P_{\mathrm{Laser}}) = \sum_{P_\gamma} \int dy\, N(y, E_{e2}, E_{\mathrm{Laser}}, P_{e2}, P_{\mathrm{Laser}}, P_\gamma)\sigma_{(e\gamma \to eH)}(s, P_{e1}, P_\gamma),$$

  - Photon beam has a energy band

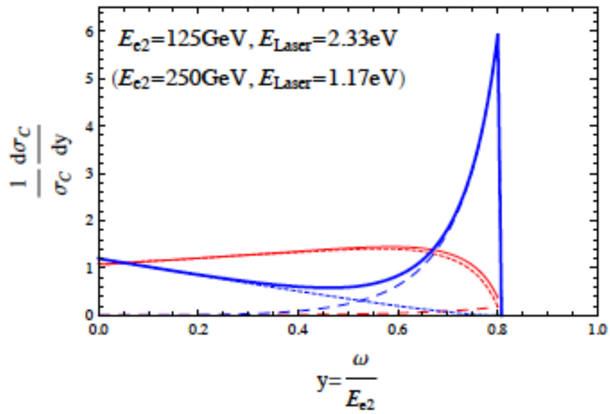

  - We study Higgs production through $b\bar{b}$ decay channel

  - Main backgrounds

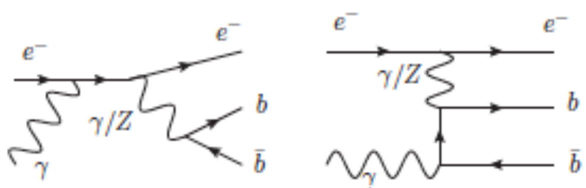

6. Numerical analysis

$$\sqrt{s_{ee}} = E_{e1} + E_{e2} = 2E_{e1}$$

$$s = y s_{ee}$$

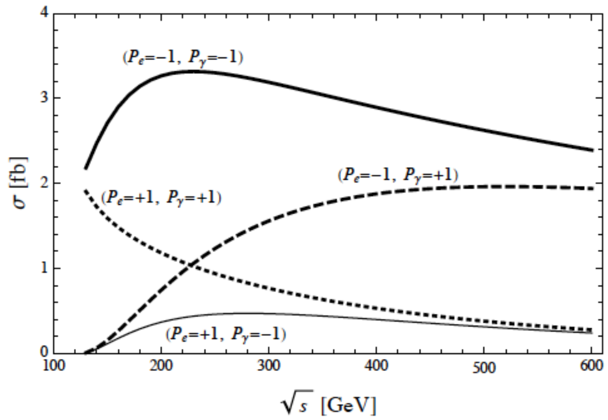

$\sqrt{s_{ee}}$ GeV	P_{e1}	P_{Laser}	σ_{cut} fb	$S/\sqrt{B}$
250	1	-1	0.50	6.17
	1	1	0.36	4.48
	-1	-1	0.80	4.51
	-1	1	1.53	8.68
500	1	-1	0.11	2.93
	1	1	0.19	1.31
	-1	-1	1.22	10.6
	-1	1	1.01	6.8

7. Summary

- Higgs production in $\mathbf{e}^{-}\gamma$ collision was investigated in SM.
- The EW one-loop contributions to the amplitude $e+\gamma \Longrightarrow e+H$ were obtained in analytical form.
- Numerical analysis was performed:
  - Contribution of $\gamma\gamma$ -fusion diagrams is dominant for $\sqrt{\mathbf{s}} < \mathbf{250\ GeV}$
  - Contributions of $\gamma\gamma$ -fusion diagrams, $\mathbf{Z}\gamma$ -fusion diagrams and W-related diagrams become the same order at larger $\sqrt{s}$
  - Contribution of Z-related diagrams is extremely small and can be neglected

  - The feasibility to find Higgs in $\mathbf{e}^{-}\gamma$ collision was studied in $e+\gamma \rightarrow e+b+\bar{b}$ channel
- This work is now in preparation.

Thank you for your attention